Molecular Vision 2015; 21:955-973 <http://www.molvis.org/molvis/v21/955>
Received 29 June 2015 | Accepted 26 August 2015 | Published 28 August 2015

Chromatin features, RNA polymerase II and the comparative expression of lens genes encoding crystallins, transcription factors, and autophagy mediators

Jian Sun,[1,2] Shira Rockowitz,[2] Daniel Chauss,[3] Ping Wang,[4] Marc Kantorow,[3] Deyou Zheng,[2,4,5] Ales Cvekl[1,2]

[1]Department of Ophthalmology and Visual Sciences, Albert Einstein College of Medicine, Bronx, NY; [2]Department of Genetics, Albert Einstein College of Medicine, Bronx, NY; [3]Department of Biomedical Science, Florida Atlantic University, Boca Raton, FL; [4]Department of Neurology, Albert Einstein College of Medicine, Bronx, NY; [5]Department of Neuroscience, Albert Einstein College of Medicine, Bronx, NY

Purpose: Gene expression correlates with local chromatin structure. Our studies have mapped histone post-translational modifications, RNA polymerase II (pol II), and transcription factor Pax6 in lens chromatin. These data represent the first genome-wide insights into the relationship between lens chromatin structure and lens transcriptomes and serve as an excellent source for additional data analysis and refinement. The principal lens proteins, the crystallins, are encoded by predominantly expressed mRNAs; however, the regulatory mechanisms underlying their high expression in the lens remain poorly understood.

Methods: The formaldehyde-assisted identification of regulatory regions (FAIRE-Seq) was employed to analyze newborn lens chromatin. ChIP-seq and RNA-seq data published earlier (GSE66961) have been used to assist in FAIRE-seq data interpretation. RNA transcriptomes from murine lens epithelium, lens fibers, erythrocytes, forebrain, liver, neurons, and pancreas were compared to establish the gene expression levels of the most abundant mRNAs versus median gene expression across other differentiated cells.

Results: Normalized RNA expression data from multiple tissues show that crystallins rank among the most highly expressed genes in mammalian cells. These findings correlate with the extremely high abundance of pol II all across the crystallin loci, including crystallin genes clustered on chromosomes 1 and 5, as well as within regions of "open" chromatin, as identified by FAIRE-seq. The expression levels of mRNAs encoding DNA-binding transcription factors (e.g., Foxe3, Hsf4, Maf, Pax6, Prox1, Sox1, and Tfap2a) revealed that their transcripts form "clusters" of abundant mRNAs in either lens fibers or lens epithelium. The expression of three autophagy regulatory mRNAs, encoding Tfeb, FoxO1, and Hif1α, was found within a group of lens preferentially expressed transcription factors compared to the E12.5 forebrain.

Conclusions: This study reveals novel features of lens chromatin, including the remarkably high abundance of pol II at the crystallin loci that exhibit features of "open" chromatin. Hsf4 ranks among the most abundant fiber cell-preferred DNA-binding transcription factors. Notable transcripts, including Atf4, Ctcf, E2F4, Hey1, Hmgb1, Mycn, RXRβ, Smad4, Sp1, and Taf1 (transcription factors) and Ctsd, Gabarapl1, and Park7 (autophagy regulators) have been identified with high levels of expression in lens fibers, which suggests specific roles in lens fiber cell terminal differentiation.

Genome-wide studies provide unbiased opportunities to better understand the molecular mechanisms of gene control. The source data include quantitative mapping of transcriptional units, including mRNAs and ncRNAs, by RNA-seq and the identification of DNA-binding transcription factors, their co-activators (e.g., chromatin remodeling complexes), RNA polymerase II (pol II), histone post-translational modifications (PTMs), and DNA methylation by ChIP-seq and similar methods. The integration of individual data and their analysis result in a comprehensive understanding of chromatin structure and RNA synthesis and processing [1-3]. To achieve this, we have recently mapped the key histone PTMs, including H4K4me1, H3K4me3, H3K27ac, and H3K27me3; pol II; and the DNA-binding transcription factor Pax6 in newborn lens chromatin [4]. Several RNA-seq studies have recently been conducted using newborn mouse lenses microdissected into the lens epithelium and lens fibers [4,5] and E13 chicken lenses microdissected into central anterior lens epithelium, equatorial epithelium, cortical fibers, and central fibers [6]. Genome-wide studies of mRNAs more abundant in embryonic lens compared to whole embryonic tissue yielded data that led to the establishment of a powerful iSyTE database enriched for lens disease-causing genes [7]. This database and other emerging data can be further mined either by mapping additional features of chromatin, additional computational re-analyses beyond the original studies, and/or a combination of both approaches.

Correspondence to: Ales Cvekl, Albert Einstein College of Medicine, 1300 Morris Park Avenue, Bronx, NY 10461; Phone: (718) 430-3217, FAX: (718) 430-8778; email: ales.cvekl@einstein.yu.edu

Numerous studies have shown that promoters and enhancers are accessible to nuclease digestion in vivo. This accessibility is thought to reflect less compacted chromatin and the presence of nucleosome-free regions [3]. Genome-wide "open" chromatin structure can be mapped using multiple approaches [3], including FAIRE-seq [8-10], DNaseI-seq [11], MNase-seq [12], and ATAC-seq [13,14]). FAIRE-seq [10] is based on earlier findings of nucleosome-free regions that may encompass as much as 2% of the genome [15]. These nucleosome-free regions, with an average size of 149 bp in length, represent platforms where clusters of multiple DNA-binding transcription factors are frequently located. Thus, the identification of nucleosome-free regions aids in the identification of transcription factors that might occupy these regions.

Lens development is an excellent model system for studying gene regulation, chromatin structure, and the degradation of subcellular organelles, as both the nuclei and mitochondria need to be degraded in terminally differentiated primary lens fibers [16-18]. A hallmark of lens fiber cell differentiation is a high level of crystallin gene expression [19], but the expression levels of crystallins related to other highly transcribed genes in different tissues have not been compared. In addition, the chromatin structure of crystallin loci remains poorly understood. Although a basic set of DNA-binding transcription factors that regulate crystallin gene expression has been identified [20,21], further studies are required to evaluate nucleosome-free regions and the distribution of pol II at the genome-wide level. Similarly, an analysis of genome-wide data pertinent to the expression of DNA-binding transcription factors and regulators of fiber cell-specific processes, such as the degradation of the subcellular organelles, should reveal novel features of the transcriptional control of these important families of genes and provide critical information for selecting the best candidates for future genetic studies of lens differentiation.

In this study, we conducted FAIRE-seq analysis of lens chromatin and integrated these data with histone PTMs and pol II occupancy. Our data establish αA-crystallin (*Cryaa*) as the most expressed gene in lens epithelium and as one of the most highly expressed genes in the mammalian body. Our data demonstrate a remarkable pol II abundance across the transcribed and frequently duplicated crystallin genes. The expression of crystallins in lens fibers is quantitatively comparable to hemoglobin gene expression in red blood cells. Additionally, among the DNA-binding transcription factors, Hsf4 expression is most highly enriched in the lens fiber cells. Finally, we found that the most abundant transcription factors are those with well-established roles in lens development and differentiation.

METHODS

RNA data analysis: The RNA-seq data were downloaded from the Gene Expression Omnibus (GEO) with the following accession numbers: erythrocytes (GSM1464982 and GSM1464983), liver (GSM1002564, GSM1182941, GSM1182942, and GSM1182943), neurons (GSM818951), and pancreas (GSM543645, GSM543646, GSM543646, GSM1002565, GSM1002566, GSM1611337, GSM1611338, GSM1611339, GSM1611340, and GSM1150322). Lens fiber, lens epithelium, and forebrain RNA-seq data were described in our previous study (GSE66961 [4]). All RNA-seq reads were processed as described in our previous publication [4], using the software Tophat/Cufflink [22-24] to determine gene expression level as reads per kilobase per million mapped reads (RPKM) [25]. We used the pre-computed RPKM values if they were available in the GEO. Chicken RNA-seq data are from GSE53976 data sets [6].

FAIRE-seq and analysis: The FAIRE experiments were performed following a protocol published by Giresi et al. [26]. Briefly, 300 newborn mouse lenses (CD-1 strain) were fixed with 1% formaldehyde for 10 min at room temperature, and the crosslinking was stopped by adding 2.5 M glycine to reach a final concentration of 125 mM. The crosslinked tissues were homogenized in a Dounce glass homogenizer (pestle B) in 10 ml of ice-cold lysis buffer (10 mM Tris-HCl pH 7.5, 10 mM NaCl, 3 mM $MgCl_2$, 0.5% NP-40) and incubated on ice for 10 min. Following centrifugation (4 min at 1,500 ×g), the pellet was re-suspended in 3 ml of sonication buffer (0.1% SDS, 10 mM EDTA, 50 mM Tris-HCl pH 8.0, proteinase inhibitor cocktail) and sheared by sonicator. Following centrifugation (1 min at 10,000 ×g), the supernatant was transferred to a new 1.5 ml test tube. Next, 300 µl of chromatin samples were treated by phenol/chloroform extraction to recover DNA not bound by nucleosomes found in the water phase. The recovered DNA were subsequently treated with RNase A (final concentration of 50 µg/ml), purified using a MinElute PCR purification kit (Qiagen, Valencia, CA), and used for subsequent Illumina sequencing library preparation. The FAIRE-seq reads were aligned to the mouse genome using Bowtie software [27], and MACS software (version 2 [28]) was used for calling peaks. Two biologic replicates of FAIRE-Seq were conducted. Analyzing the genome-wide read distribution (counting reads in 5-kb windows), we found the two replicates were significantly correlated (Pearson correlation coefficient = 0.89). For simplicity, we present data from one replicate

(GEO accession number, GSM1841114) deposited within the GSE66961 data set.

RNA polymerase II ChIP-seq and RNA-seq data sets: The pol II peak identification and RNA-seq data have been described elsewhere [4]. Chicken RNA-seq data are from GSE53976 data sets [6].

DNA-binding transcription factors and autophagy: The lists of DNA-binding transcription factors and autophagy genes were downloaded from AmiGO2.

RESULTS AND DISCUSSION

Crystallins, hemoglobins, and Cacna2d1 are the most abundant transcripts in differentiated mammalian cells: Lens crystallins have been identified as the most abundant transcripts in the mouse lens by RNA-seq [5]; however, it is unknown how their expression ranks among genes highly expressed in terminally differentiated cells. To address this issue, we examined transcriptomes obtained from mouse lens epithelium, lens fibers, erythrocytes, forebrain, liver, neurons, and pancreas generated by RNA-seq [4,29-32]. Individual transcript abundance was determined from normalized reads per kilobase per million mapped reads (RPKM). Next, to compare the expression of top expressed genes across tissues, we selected the 10 most abundant transcripts in each tissue/organ and computed the ratios of their expression to the median expression level of all transcribed genes in the same tissue/organ, resulting in a relative "fold change" over the median (log2 scale). In Figure 1, we present the data for the top 10 lens fiber cell transcripts and the top five transcripts each from lens epithelium, erythrocytes, the forebrain, the liver, neurons, and the pancreas. This analysis revealed that five hemoglobin-encoding mRNAs (Hbb-bs, Hbb-b1, Hbb-b2, Hbb-bt, and Hba-a2) in red blood cells; calcium channel, voltage-dependent, α2/δ subunit 1 (Cacna2d1) in neurons; and 10 crystallins (Cryga, Cryge, Crygb, Cryba1, Crybb3, Cryaa, Crybb1, Crygd, Cryba4, and Cryba2) in lens fiber cells represent a group of the most abundant transcripts, followed by insulins (Ins2 and Ins1) and glucagon (Gcg) in the pancreas (Figure 1). In lens epithelium, the most abundant transcripts were in the order of Cryaa > Crybb3 > Rprl3 > Rn45s > Cryba1 (Figure 1). Taken together, these data quantitatively establish that in lens fiber cells, crystallins reach such prominent expression levels that they can only be compared with the adult hemoglobin genes in erythrocytes and calcium channel transcripts encoding Cacna2d1 in neurons.

A known common denominator between lens crystallins, insulin, and glucagon (Figure 1) is that these genes share common transcription regulators, including Pax6 and large Maf proteins. Interestingly, Prox1, another transcriptional regulator of crystallins [31,33,34], is also expressed in the pancreas, where it controls exocrine functions [35]. Specifically, genetic and molecular studies have established multiple roles of Pax6 and c-Maf in crystallin gene regulation [36-42]. Studies in cell culture systems added MafA and MafB [39,40], although *MafA*$^{-/-}$*; MafB*$^{-/-}$ and *MafA*$^{-/-}$*; MafB*$^{-/-}$ compound lenses appear normal [43]. In the pancreas, the loss of Pax6 results in the decreased expression of insulin, glucagon, and somatostatin [44], and numerous Pax6-binding sites have been identified in the regulatory regions of these genes [45-48]. MafA is critical for glucose-responsive insulin gene expression in β-cells [49] and is regulated by Pax6 [50]. MafB regulates glucagon gene expression [51] and is required for β-cell maturation [52]. Both glucagon and insulin promoters also bind c-Maf [53], although its global role in pancreas biology remains to be established. Finally, Pax6 has been shown to directly regulate the expression of insulin-like peptides in insulin-producing neurons in *Drosophila* [54].

We were thus intrigued to compare the expression levels of crystallins in the pancreas and of insulins and glucagon in the lens. The RNA expression analysis of lens fibers revealed increased levels of glucagon (Gcg) over the median; however, the expression of both insulin genes was significantly below the median level (Figure 2A). In pancreas cells, the expression of three crystallins, αB- (Cryab), βA2- (Cryba2), and βB3- (Crybb3), was above the median level (Figure 2B); however, these levels were significantly below the expression levels of the top 10 pancreas transcripts. From these data, we concluded that even a full complement of DNA-binding transcription factors that regulate crystallin gene expression is not sufficient to elicit their expression in pancreas cells, raising the possibility that the regulatory activities of these factors are modified by lens- and pancreas-specific signaling and/or posttranslational modifications. It is also possible that gene control of αB-, βA2-, and βB3-crystallins (Figure 2B) utilizes a different set of transcription factors compared to the lens, as shown for αB-crystallin in cardiac and muscle cells [55]. Interestingly, the upregulation of crystallins has been identified in various diabetic eye models [56,57], raising the possibility that specific pathological conditions overcome the tight control of crystallin gene expression. Alternatively, it remains possible that individual crystallin gene expression in pancreas requires additional DNA-binding transcription factors, such as Hsf4 (see below), weakly expressed in the pancreas [58].

Crystallin loci are marked by reduced nucleosomal density ("open" chromatin) and a high abundance of RNA polymerase II: It has previously been shown that there is a correlation between chromatin structure and transcription

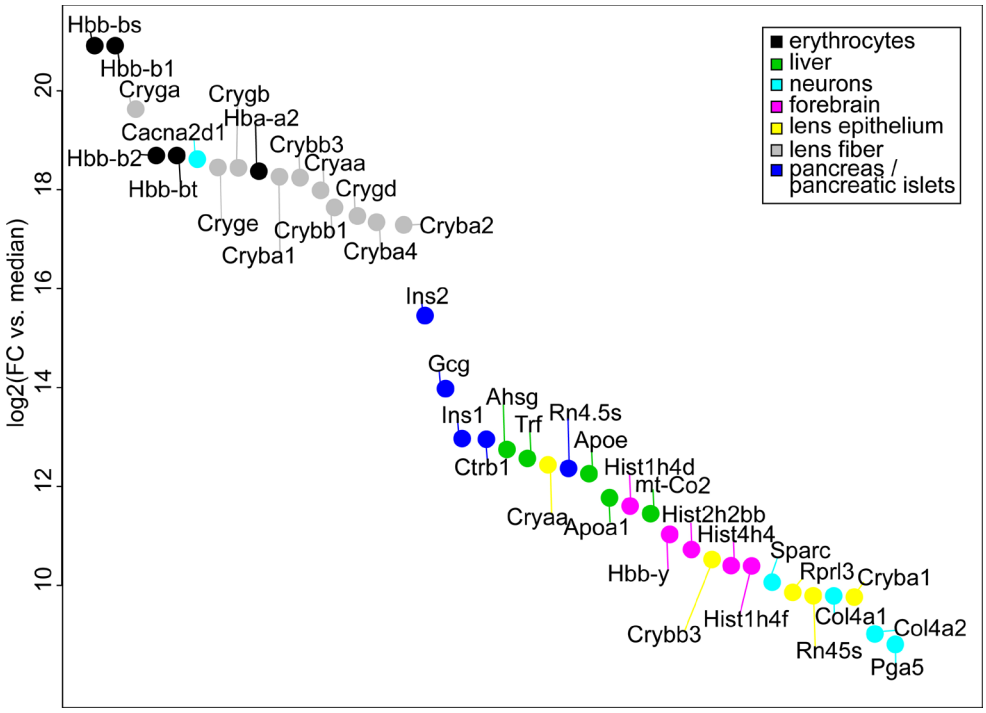

Figure 1. Top expressed genes in terminally differentiated mammalian tissues and organs. The y-axis shows the relative expression levels (*versus* the median expression level of protein coding genes in the tissue) of the top 10 expressed genes in each tissue. Individual colored dots represent transcripts from different tissues: erythrocytes (black), liver (green), neurons (light blue), forebrain (purple), lens epithelium (yellow), lens fibers (gray), and pancreas/pancreatic islets (dark blue). Hbb-bs (β^S-globin, adult s chain), Hbb-b1 (β^A-globin adult major chain), Cryga (γA-crystallin), Hbb-b2 (β^A-globin adult minor chain), Hbb-bt (β^A-globin adult t chain), Cacna2d1 (calcium channel, voltage-dependent, α2/δ subunit 1), Cryge (γE-crystallin), Crygb (γB-crystallin), Hba-a2 (α^A-globin adult chain 2), Crybа1 (βA1-crystallin), Crybb3 (βB3-crystallin), Cryaa (αA-crystallin), Crybb1 (βB1-crystallin), Crygd (γD-crystallin), Cryba4 (βA4-crystallin), Cryba2 (βA2-crystallin), Ins2 (insulin II), Gcg (glucagon), Ins1 (insulin I), Ctrb1 (chymotrypsinogen B1), Ahsg (α-2-HS glycoprotein), Trf (transferrin), Rn4.5s (4.5S RNA), Apoe (apolipoprotein E), Apoa1 (apolipoprotein A-1), Hist1h4d (histone cluster 1, H4d), mt-Co2 (cytochrome c oxidase II, mitochondrial), Hist2h2bb (histone cluster 2, H2bb), Hbb-y (hemoglobin Y, β-like embryonic chain), Hist4h4 (histone cluster 4, H4), Sparc (osteonectin), Rprl3 (RNase P RNA-like 3), Rn45s (45S pre-rRNA), Col4a1 (collagen, type IV, alpha 1), Col4a2 (collagen, type IV, alpha 2), and Pga5 (pepsinogen 5, group I).

levels [59,60]. Because the expression of crystallins in lens fibers reaches an exceptional level, we wanted to map the nucleosome density using FAIRE-seq (see the Materials and Methods section) and correlate the data with pol II occupancy and transcription output measured by RNA-seq analysis. Examining the global distribution of the FAIRE-seq signal, we found extended open chromatin regions encompassing crystallin loci located on the mouse chromosomes 1, 5, 9, 11, 16, and 17, often as clusters of duplicated genes (Figure 3). Many of those loci also contained a high abundance of pol II, especially at the *Cryaa* locus. While the overwhelming majority of pol II occupancy was found at the crystallin loci, a large enrichment was also observed in a few additional loci on chromosomes 2 and 19 (Figure 3), including *Lrrc4c* and lncRNA *Malat1* regions.

We identified 107,737 FAIRE-seq peaks using MACS2 software [28], ranging from 133 bp to 5,374 bp and totally covering ~37 Mb of the mouse genome (Table 1). Based on the refSeq annotation, 5.6% of the peaks were mapped to promoters (+/− 2 kb of the annotated transcription start sites) and 52.9% of the peaks were within 50 kb of the annotated genes. To better link open chromatin with gene regulation, we compared and integrated the FAIRE-seq data with other chromatin modification data. Previously, we identified a total of 301 regions with extended H3K27ac enrichment in lenses [4] using the recently described method ("ROSE") for identifying "super enhancers" [61]. For comparison, 308 super enhancers were found in the embryonic forebrain chromatin (Table 1). We found 420 FAIRE-seq peaks within the 301 lens super enhancers; 190 genes were found to within 50 kb of these peaks using GREAT software [62], and the involved genes were significantly enriched for functions related to both eye development and eye diseases (Appendix 1). On the reverse side of the "super enhancer" analysis, we analyzed extended H3K27me3 blocks (>15 kb) and more specifically those extending beyond the start and end of the annotated genes (Table 1). A total of 164 such extended regions ("super repressors") were found in the lenses, covering 237 genes, of which 99 encode well-studied transcription factors that control patterning and terminal differentiation, such as Myod1, Neurod1, Hand1, and 29 Hox genes. The repression of these genes is strongly supported by their low expression values in the global RNA-seq data (data not shown). Nevertheless,

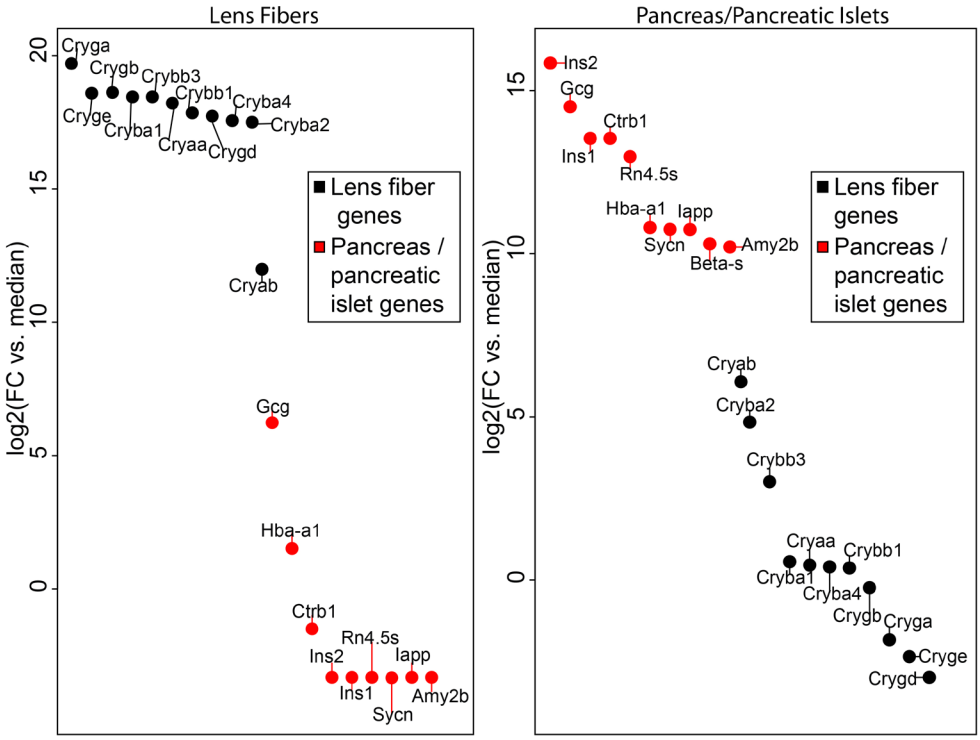

Figure 2. Gene expression comparison between lens fibers and pancreas/pancreatic islets. **A**: Visualization of expression levels of top expressed genes in lens fibers (n=10, Cryab also included as it is the most abundant crystallin in the pancreas, black circles) and pancreas genes (red circles). **B**: Expression levels of top expressed genes in the pancreas (n=10, red circles) and lens crystallins (black circles). The data were calculated as described in the legend for Figure 1.

113 FAIRE-seq peaks were located within these super repressors. As expected, they were significantly enriched at loci encoding transcription factors (e.g., *Lhx3* and *Otx2*) involved in cell fate commitment and system development, including eye development.

Transcriptional regulation of the mouse αA-crystallin (*Cryaa*) locus has been deciphered using a combination of transgenic mouse and molecular biology studies, leading to the identification of two distal developmentally controlled enhancers within a 16 kb genomic region [63-66]. In the *Cryaa* locus (chromosome 17), prominent pol II enrichment is found in the coding gene sequences and the extended 3′-UTR (Figure 4A). In contrast, the *Cryab* gene is located in the head-to-head orientation with *Hspb2* (chromosome 9, Figure 4B). The transcription start sites of *Cryab* (in the lens) and the sequence-related *Hspb2* differ by only 866 bps; however, only the *Cryab* gene is expressed in the lens [67,68]. Interestingly, the *Cryab* regulatory regions are extended to a 4 kb 5′-flanking region encompassing the *Hspb2* gene [69]. As there is pol-II detected in the 5'-region of Cryab, including the coding regions of *Hspb2*, it appears that there are multiple upstream start sites of Cryab gene transcription [67-69]. In the forebrain, we did not find any significant numbers of αA- and αB-crystallin transcripts; nor did we observe pol-II enrichment at these loci (Figure 4A,B).

The mouse chromosome 1 contains a cluster of five *γ-crystallin* genes (*Cryga-Cryge*) separated by ~0.8 Mbp genomic region, where the sixth member, *Crygf*, is located in the opposite orientation relative to the *Cryga-Cryge* cluster (Figure 4C). In the *γ-crystallin* cluster, pol II is localized in both the transcribed regions (as expected) and the intergenic regions linking these genes (Figure 4C). This suggests the possibility that the enzyme leaving the template can be "recycled" by the next transcriptional unit without "leaving" the active chromatin domain. Mouse chromosome 5 harbors five *β-crystallin* genes: *Cryba4*, *Crybb1*, *Crybb2*, *Crybb3* (Figure 4D,E), and *Crygn* (data not shown). The *Cryba4* and *Crybb1* are assembled in a head-to-head orientation and are expressed both in lens fibers and lens epithelium (Figure 4D). There are six non-crystallin genes between the *Cryba4* and *Crybb1* pair and a pair of *Crybb2* and *Crybb3* genes. Both Cryba4 and Crybb1 are expressed in lens fibers and epithelium (Figure 4D). The spacer region of 3.3 kb between *Cryba4* and *Crybb1* does not harbor any appreciable amount of pol II (Figure 4D). In contrast, Crybb2 is not yet transcribed (Figure 4E) compared to Crybb3 in newborn mouse lenses (Figure 1 and Figure 4E), as Crybb2 expression is augmented after the birth [70]. Note that in E12.5 forebrain chromatin, the αA- and γF-crystallin encoding mRNAs are of low abundance [4]. From these data, we concluded that crystallin loci are marked as open chromatin. Very high levels of crystallin gene

Table 1. Summary of FAIRE-seq data in newborn lens chromatin*).

Chromatin modification/Pol II/Pax6	Forebrain			Lens		
	Peak Number	Total Base Pairs	Enhancer [%]	Peak Number	Total Base Pairs	Enhancer [%]
FAIRE-seq				107,737	38,986,091	47.3%
"Super-enhancer"	308	7,148,537	100.0%	301	4,624,444	100.0%
"Super-enhancer" AND Pax6	97		31.5%	112		37.2%
"super-repressor" >15 kb H3K27me3	412	14,603,188	100.0%	164	4,891,836	100.0%
"super-repressor" >15 kb H3K27me3 AND Pax6	60		14.6%	8		4.9%

*)The data on "super-enhancers" were reported elsewhere [4] and are shown here for comparisons

expression correlate with an extremely high abundance of pol II all across the individual transcriptional units. Ongoing experiments are focused on discovering if these crystallin transcriptional units form "transcriptional hub/factories" in the 3D nuclear space [71,72].

Transcription factors enriched in lens epithelium and lens fibers: Although an appreciable number of DNA-binding transcription factors have been studied during lens differentiation, with notable differences in their expression domains in the lens [18,73], an unbiased analysis of transcripts encoding

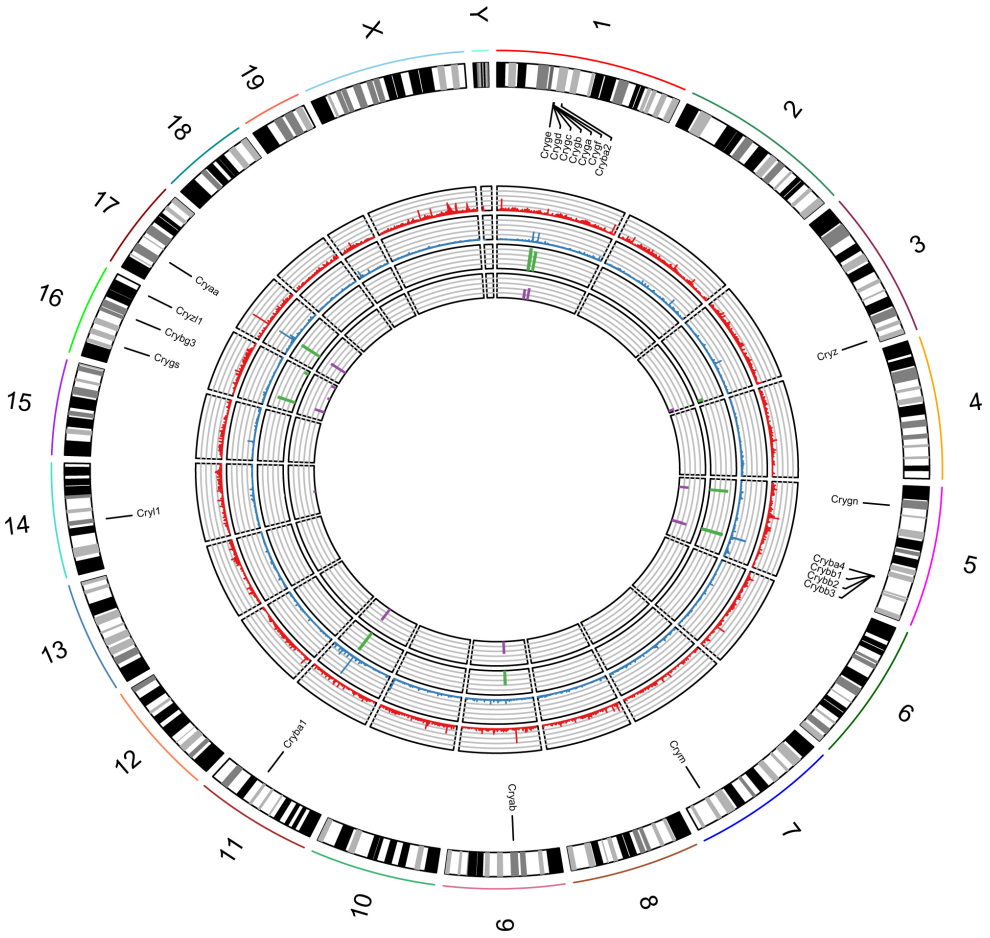

Figure 3. Rcircos [120] diagram showing "open" chromatin and highly active transcription at many crystallin loci, particularly at the Cryaa. The circles (outermost to innermost) are genome-wide lens FAIRE-seq read density (red), lens pol II ChIP-seq read density (blue), and expression levels (RPKMs) of crystallin genes in lens fibers (green) and lens epithelium (purple). Signals from input lens chromatin have been subtracted for the FAIRE-seq and ChIP-seq data.

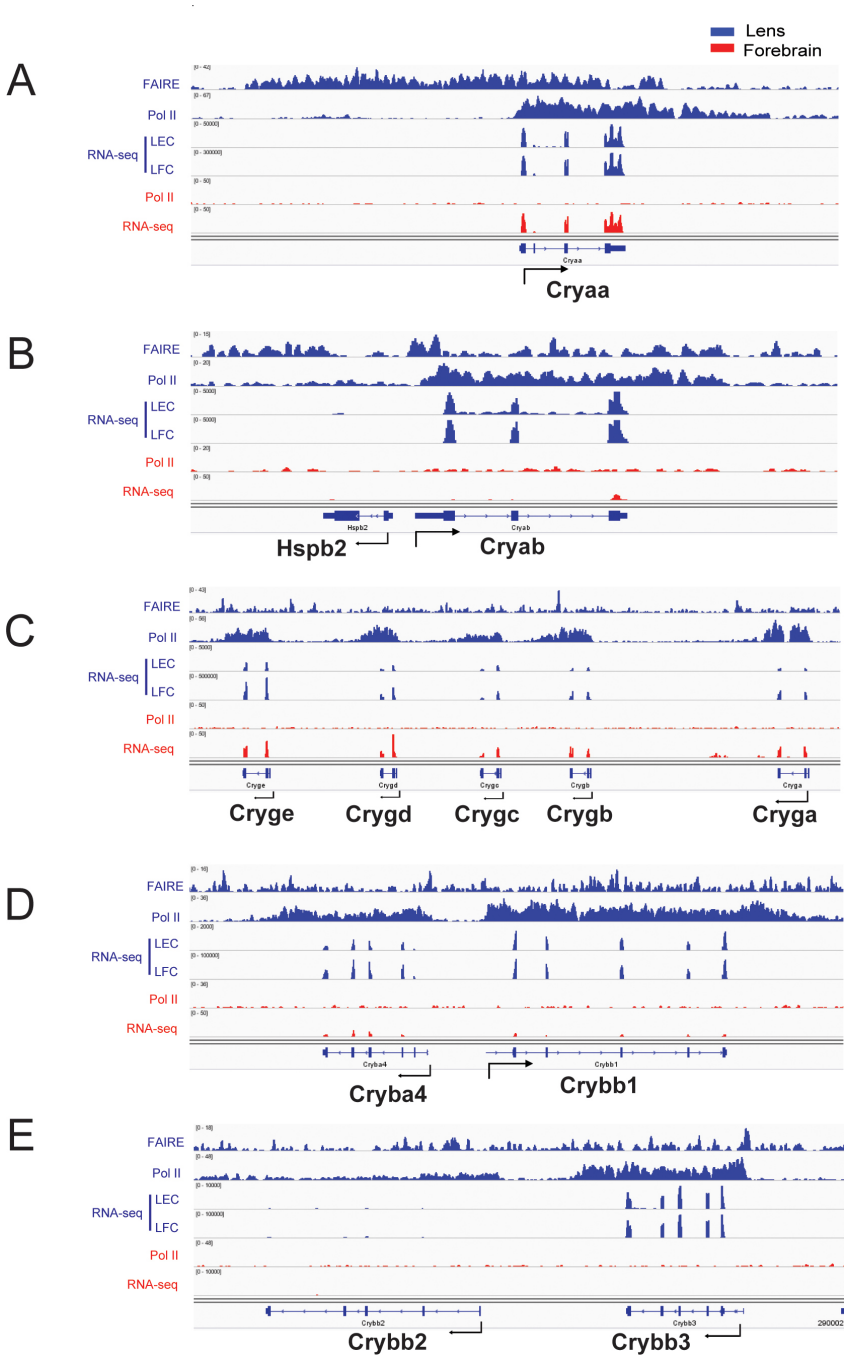

Figure 4. Chromatin structure and RNA visualization of representative mouse crystallin genes. **A**: *Cryaa* (chromosome 17, length of region shown: 40 kb). **B**: *Cryab-Hspb2* (chromosome 9, length of region shown: 20 kb). **C**: A cluster of six *γ-crystallin* genes and *βA2-crystallin* (*Cryba2*) is present on chromosome 1. A 100 kb region encompassing five genes, including *Cryga*, *Crygb*, *Crygc*, *Crygd,* and *Cryge*, is shown. **D**: *Cryba4-Crybb1* (chromosome 5, length of region shown: 40 kb). E) *Crybb2-Crybb3* (chromosome 5, length of region shown: 40 kb). Tracks: Lens (FAIRE-seq, pol II, RNA-seq), forebrain (pol II and RNA-seq). Lens epithelium, LEC; lens fiber cells, LFC.

transcription factors enriched in the lens epithelium and lens fibers has not yet been conducted. Here, we analyzed lens transcriptomes using three pair-wise comparisons: lens epithelium versus embryonic forebrain, lens fibers versus embryonic forebrain, and lens fibers versus lens epithelium. The embryonic E12.5 forebrain was included for comparison as both the lens and the forebrain are of common ectodermal origin and both tissues require Pax6 for their formation

[18,74]. Furthermore, the analysis of transcript abundance between tissues greatly aids in the identification of functional and disease-related genes [7]. The transcripts identified as being more abundant in lens epithelium than in the forebrain include Tfap2a (AP-2α), Foxe3, Pitx3, and Prox1 (Figure 5A), while Pitx3, Hsf4, Prox1, and Maf (c-Maf) are more abundant in lens fibers (Figure 5B). The most notable lens fiber-enriched transcripts include Hsf4, Maf, Sox1, and Prox1 (Figure 5C). In contrast, compared to lens fibers, lens epithelium is enriched for Pax6, Jun, Foxe3, and Hey2 transcripts (Figure 5C). In both lens compartments, Ctnnb1 (β-catenin) and Atf4 show very high levels of expression, consistent with their roles in lens differentiation [75-77]. It should be noted that only a fraction of cellular β-catenin is engaged in transcription through the canonical Wnt/β-catenin signaling pathway [78].

Our previous analysis of Pax6 and Prox1 identified novel distal enhancers of both genes [4]. Here, we show chromatin data regarding selected genes that represent the most abundantly expressed transcription factors in the lens (Tfap2a, Hsf4 and Maf), that are expressed highly in the lens and forebrain (Ctnnb1), that are expressed in lens epithelium and the forebrain (Sox2), and that are expressed highly in the forebrain (Sox11; Figure 6 and Figure 7). Both Tfap2a and Foxe3 mRNAs are abundant in the lens epithelium (Figure 6A), which is in agreement with earlier studies of these transcription factors in the lens [79,80]. Both loci are marked with a much lower level of H3K27me3 in the lens compared to forebrain chromatin. Hsf4 appears to be one of the most important DNA-binding transcription factors in lens fibers [81]; it controls the expression of all γ-crystallins [58] and αB-crystallin [82]. In lens chromatin, the *Hsf4* locus is marked by low levels of H3K27me3 (Figure 6C). In contrast, the Hsf4 locus is marked by large H3K27me3 domains in the forebrain. Maf is more highly expressed in fibers than in lens epithelium [38] and is only weakly expressed in the forebrain, consistent with the differential enrichment of H3K27me3 in the *Maf* locus (Figure 6D). In lens chromatin, the *Maf* locus is marked by H3K27ac, and its promoter/gene body are also marked by H3K4me3 (Figure 6D). β-catenin (Ctnnb1) is a multifunctional protein with a specific role in transcription; Wnt signaling stimulates the translocation of β-catenin into the nucleus, where it forms a specific complex with HMG box DNA-binding factors Lef/Tcf [83]. Ctnnb1 is highly expressed in the lens and forebrain, consistent with the low abundance of H3K27me3 along this gene in both tissues (Figure 7A). In addition to its role in the ES cell core Oct4-Sox2-Nanog regulatory network, Sox2 is an important regulator of lens placode formation [84-86] and neural stem cells [63,87]. The present data suggest different regulatory mechanisms of the Sox2 gene in lens epithelium and the forebrain, as the H3K4me1, H3K27ac, H3K4me3, and H3K27me3 core histone PTMs show different patterns of intensities in lens and forebrain chromatins (Figure 7B), consistent with the different utilization of tissue-specific enhancers [88]. Finally, Sox11 is expressed in the invaginating lens placode and is required for the separation of lens vesicles from the surface ectoderm [89]. Its expression is reduced in the differentiating lens [90]. The expression of Sox11 is high in the neonatal cortex [91] and is essential for embryonic and adult neurogenesis [92]. The chromatin structure of Sox11 in the forebrain is marked by abundant H3K4me1, H3K27ac, and H3K4me3, while these histone PTMs are less abundant in lens chromatin (Figure 7C).

The current analysis of the most abundantly expressed DNA-binding transcription factors in the mouse lens supports the functional roles of these proteins in controlling lens development [21,73]. It also supports the rational design of iSyTE for identifying lens disease-causing genes based on their relative abundance in the lens compared to whole embryonic tissues [7]. Many of these DNA-binding transcription factors (e.g., Atf4, Maf, Pax6, Prox1, Sox2, Tfap2a, etc.) bind CREB-binding protein (CBP) and p300 and p300 histone acetyltranferases, which are essential for embryonic lens induction [93] and display different temporal and spatial expressions in the embryonic mouse lens [94]. The loss of three CBP/p300 alleles results in cataracts [92]. Some of these factors (e.g., Gata3, Hsf4, and Pax6) interact with SWI/SNF ATP-dependent chromatin remodeling complexes [65,95].

Autophagy transcripts enriched in lens epithelium and lens fibers: Lens fiber cell differentiation and homeostasis requires the degradation of nuclei and mitochondria. Lens differentiation includes autophagy [6,96], mitophagy [97], chromatin degradation by lens-preferred DNase IIβ endonuclease [98], and proteasome-mediated protein degradation [99,100]. Here, we analyzed the expression and chromatin features of autophagy genes (Figure 8, Figure 9). Eight transcripts encoding Ctsd, Gabarapl1, Park7, Fis1, Optn, Wipi1, Wipi2, and Mtor show pro-lens expression. Ctsd is the major proteolytic enzyme and marker of catabolic activity in various ocular tissues [101,102]. Its transcripts are more abundant in the lens compared to the embryonic forebrain (Figure 8A,B). γ-aminobutyric acid (GABA) A receptor-associated protein-like 1 (Gabarapl1, Atg8l) is the mammalian homolog of yeast Atg8, which regulates autophagosome formation [103]. It is highly expressed in the lens and is more abundant in lens fibers (Figure 8C). Among all the transcripts examined, Parkinson's disease (autosomal recessive, early onset) 7 (Park7) is the most abundant transcript among the autophagy

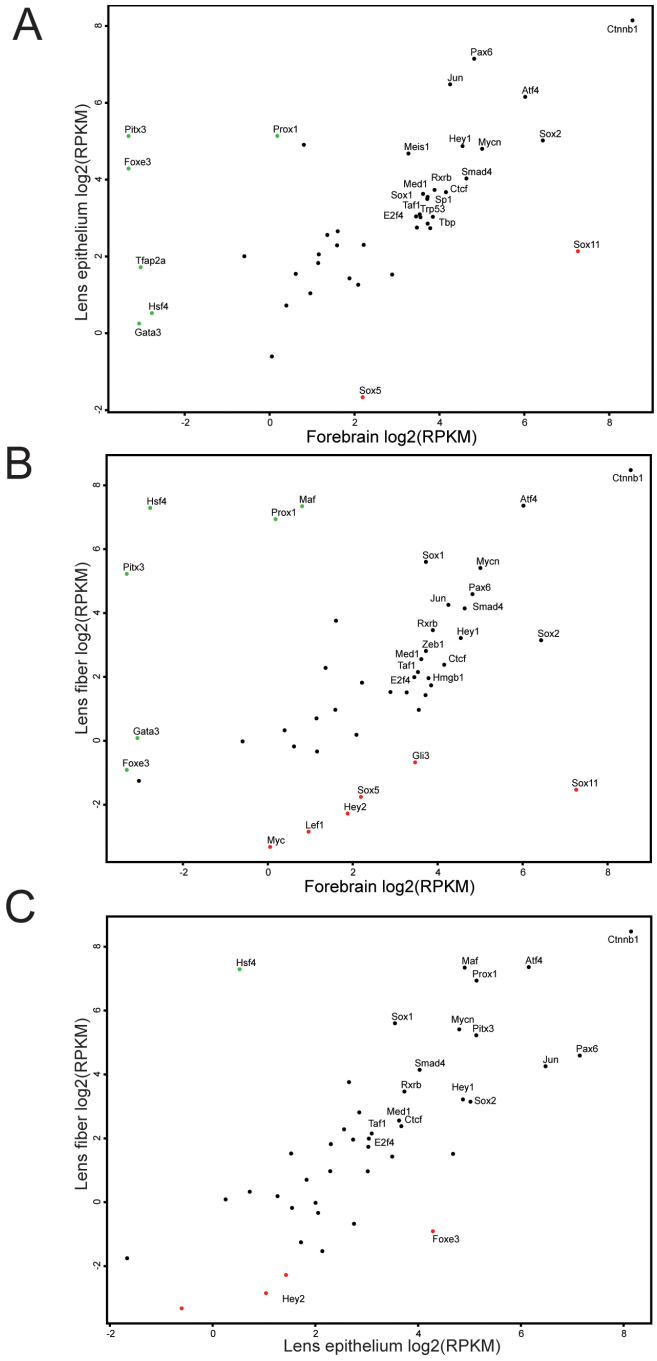

Figure 5. Differential expression of DNA-binding transcription factors that are highly expressed in lens epithelium and lens fibers. **A**: Lens epithelium versus forebrain, **B**: Lens fibers versus forebrain, **C**: Lens fibers versus lens epithelium.

group examined here (Figure 8B,C). Park7 is required for mitochondrial homeostasis and turnover [104]. The pro-fission mitochondrial Fis1 (Fission 1) is highly expressed in the lens, with a higher abundance in lens fibers (Figure 8C); it induces mitochondrial fragmentation before mitophagy [105]. Interestingly, Park7 promotes the proteosomal degradation of Fis1 [106].

Together with sequestosome 1 (SQSTM1/p62) and ubiquilin-2 (Ubgln2), optineurin (Optn) functions as an autophagy receptor protein [107]. Optn is more abundant in mouse lens fibers compared to lens epithelium (Figure 8C). The WD repeat domain, phosphoinositide interacting 1 (Wipi1, ATG18) and 2 (Wipi2, ATG18B) proteins function as essential phosphatidylinositol 3-phosphate (PtdIns3P)

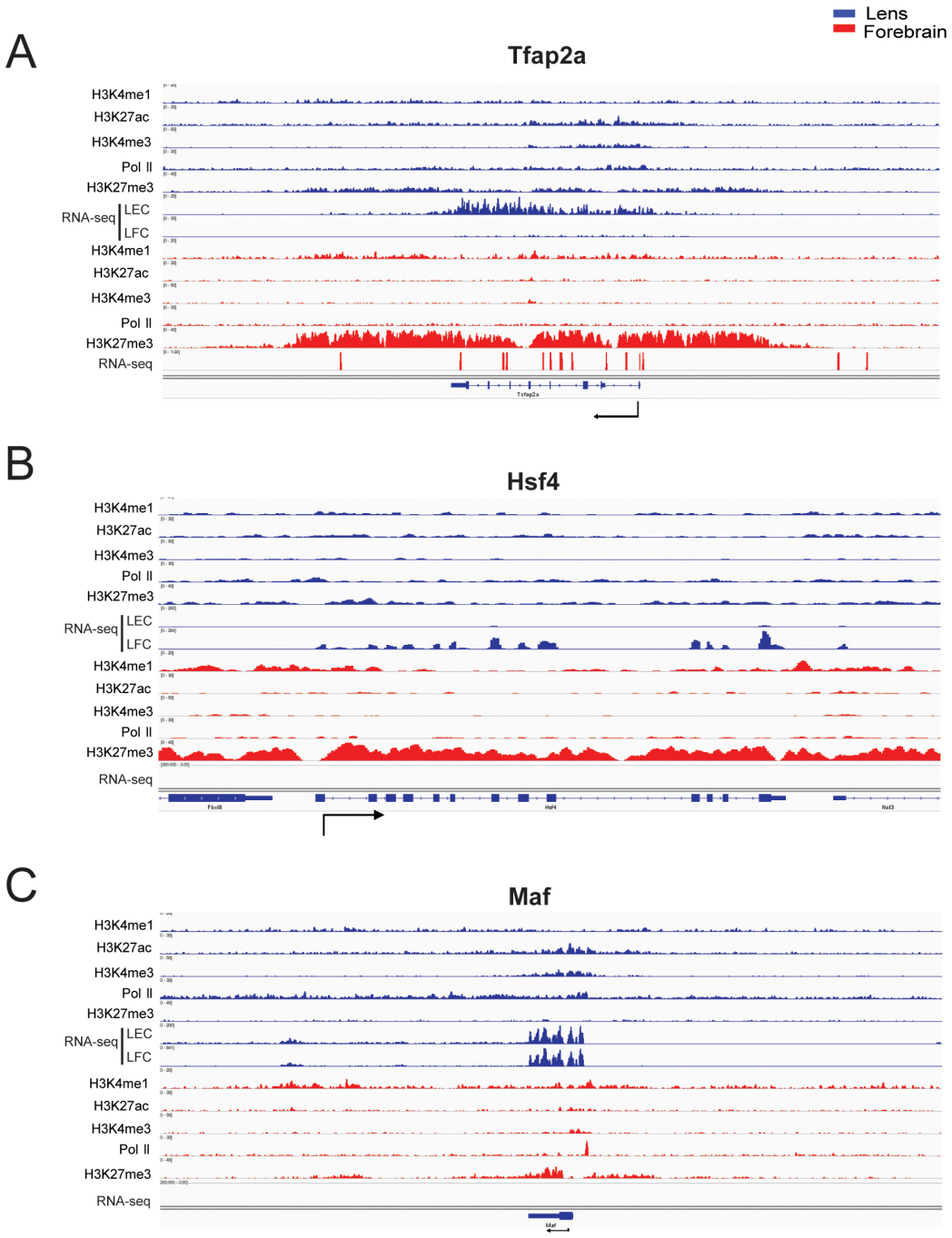

Figure 6. Chromatin structure of individual loci encoding selected lens-enriched DNA-binding transcription factors. **A**: *Tfap2a*. **B**: *Hsf4*. **C**: *Maf*. Distribution of H3K4me, H3K27ac, H3K4me3, Pol II , H3K27me3 (ChIP-seq), and RNA (RNA-seq) data are from data set GSE66961 [4].

effectors at the nascent autophagosome [108]. Both Wipi1 and Wipi2 are more abundant in lens fibers compared to the forebrain (Figure 8B). Finally, the mechanistic target of rapamycin (serine/threonine kinase; Mtor) is the central regulator of autophagy [109,110], with increased expression in lens fibers compared to the forebrain (Figure 8B), and has an established role in lens organelle degradation [96].

The transcription of autophagy genes is regulated by Tfeb [111], a subfamily of FoxO proteins, including FoxO1, FoxO3a, FoxO4 and FoxO6 [112], and Hif-1α (gene name: Hif1a) DNA-binding factors. Hif1α is regulated at multiple

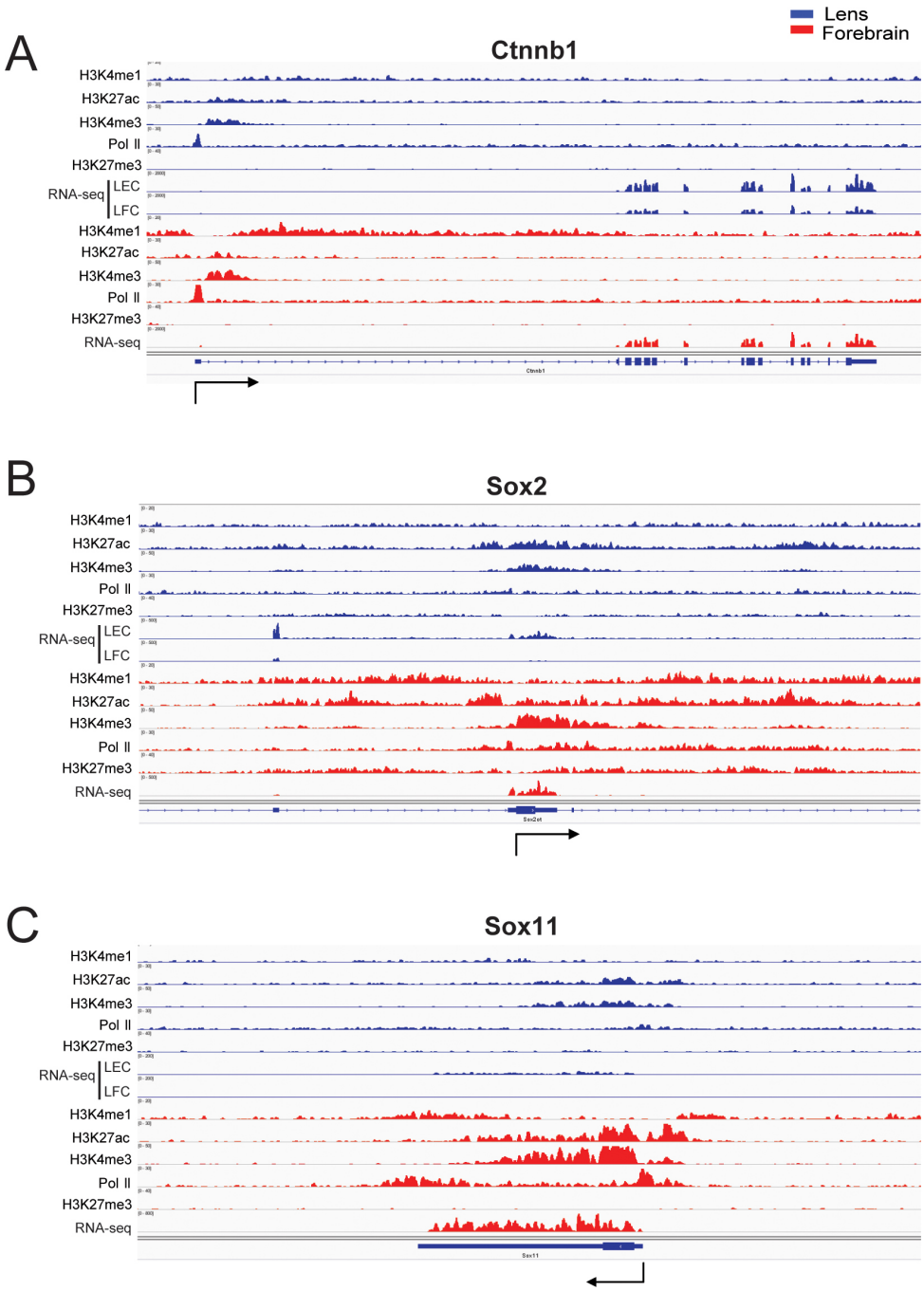

Figure 7. Chromatin structure of individual loci encoding selected forebrain- and lens-enriched transcription factors. **A**: *Ctnnb1*. **B**: *Sox2*. **C**: *Sox11*. See the legend for Figure 6 for details.

levels, as its degradation is controlled by chaperone-mediated autophagy [113] and transcriptional control of BNIP3 [114]. Here, we found increased expression of Tfeb in both lens epithelium and lens fibers relative to the forebrain (Figures 8A,B), increased expression of Hif1a in lens epithelium compared to the fibers (Figure 8C), and moderately increased expression of Foxo1 in lens epithelium compared to the E12.5 forebrain (Figure 8A). Tfeb (bHLHe35) is a helix–loop–helix DNA-binding factor and serves as a master regulator of the lysozomal gene network, lysosomal biogenesis, autophagy, and other related processes [111]. The chromatin structure of the Tfeb locus and the RNA-seq data show highly active transcription in both lens epithelium and fibers and reveal an intragenic enhancer, marked by H3K4me1 and H3K27ac

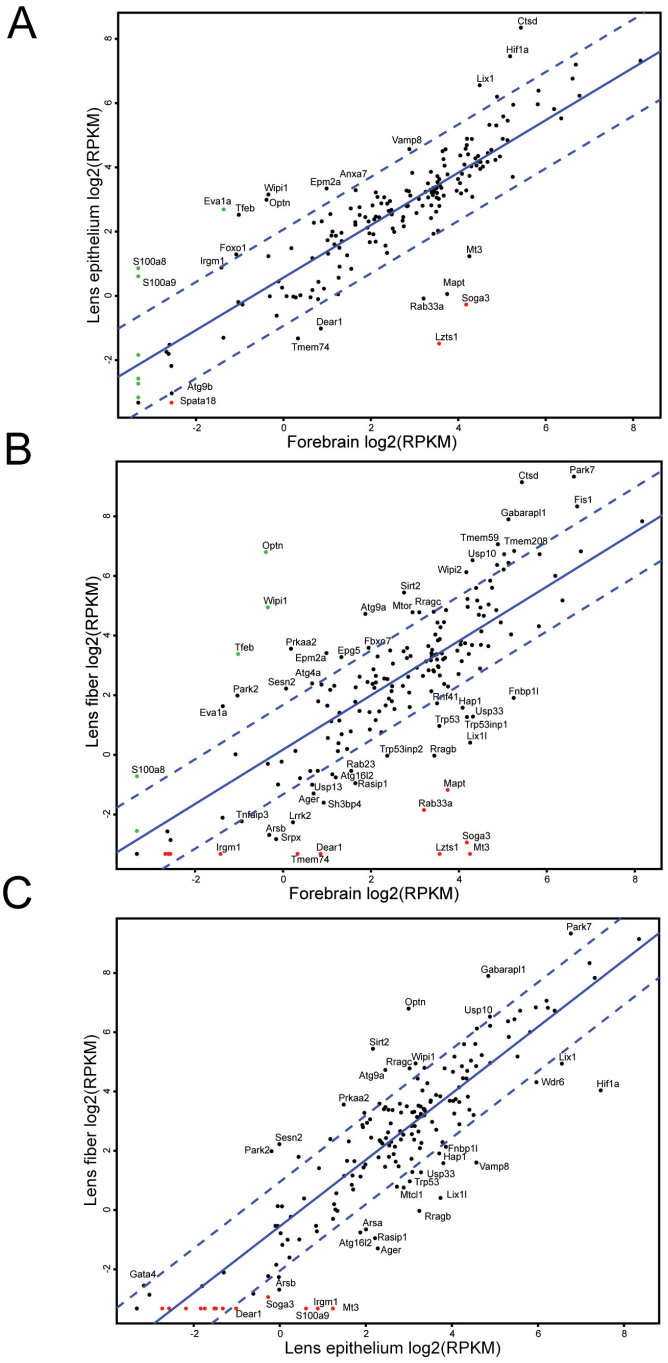

Figure 8. Differential gene expression of key autophagy and mitophagy genes. **A**: Lens epithelium versus forebrain. **B**: Lens fibers versus forebrain. **C**: Lens fibers versus lens epithelium.

(Figure 9A). RNA-seq data at Foxo1 show abundant pre-spliced RNAs in lens epithelium, raising the possibility that splicing may control the availability of the Foxo1 mRNAs (Figure 9B). Its lower level of expression in the forebrain correlates with increased H3K27me3 in the promoter region (Figure 9B). The chromatin structure of the Hif1a locus suggests that its expression is regulated by the promoter; in forebrain chromatin, pol II is abundant, although RNA-seq data show much lower levels of expression compared to the lens epithelium (Figure 9C). Taken together, the targeting of Tfeb, Foxo1, and Hif1a in the lens by MLR10-cre [115] represents excellent opportunities to determine the function of these genes in lens differentiation and subcellular organelle turnover.

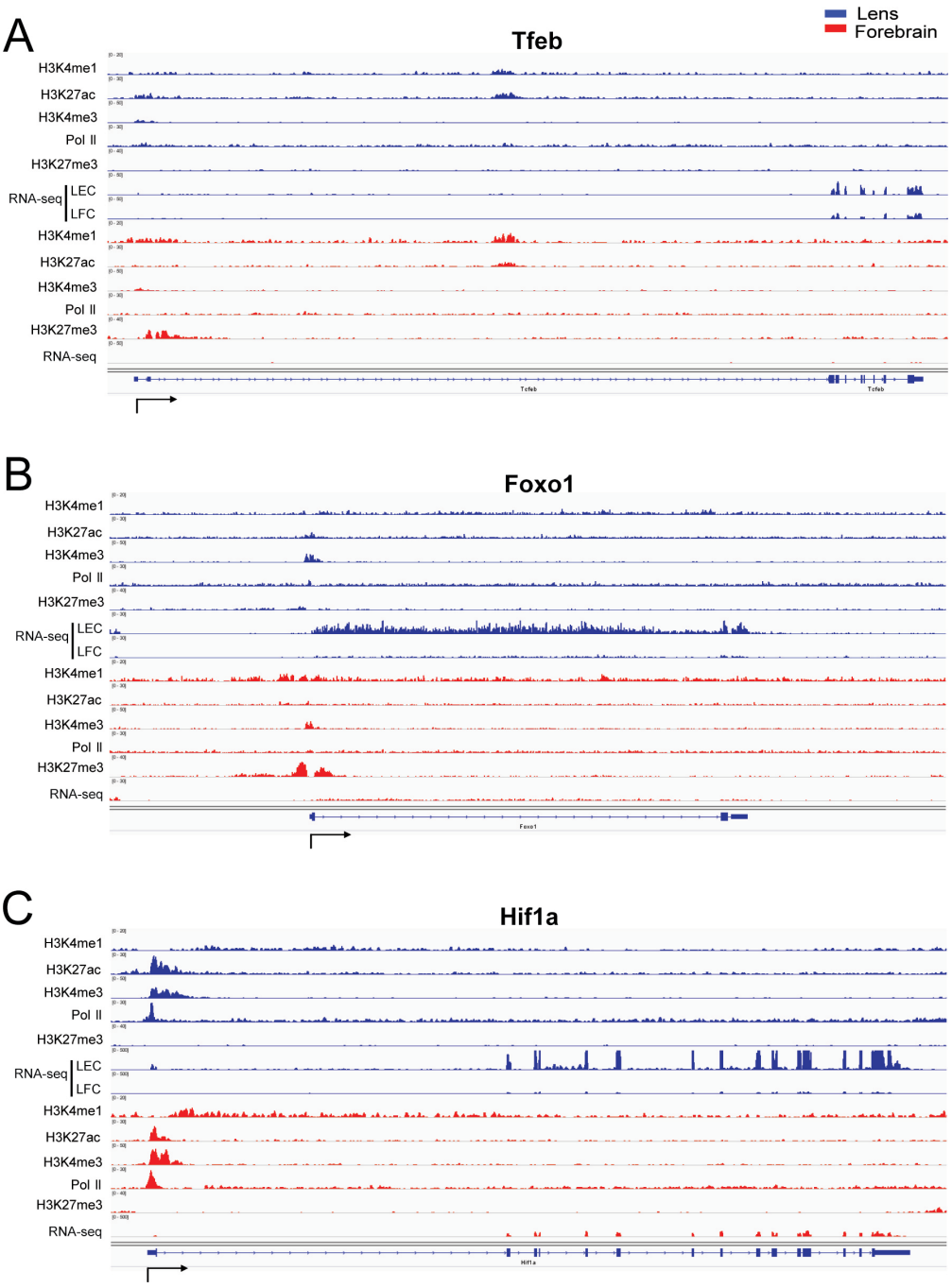

Figure 9. Chromatin structure of individual loci encoding DNA-binding transcription factors that control autophagy and mitophagy genes. **A**: *Tfeb*. **B**: *FoxO1*. **C**: *Hif1a*. See the legend for Figure 6 for details.

Four sets of transcriptome data have been generated in E13 embryonic chicken lens compartments [6]. Herein, we analyzed spatial gene expression changes of those 11 mouse genes, grouped as autophagy regulators (Figure 10A) and transcription factors (Figure 10B). Mouse Fis1 does not have any known chicken homolog. In both mouse and chicken lenses, the abundance of autophagy transcription factors is in the order Foxo1 < Tfeb < Hif1a (Figure 8, Figure 10). The chicken data show major upregulation of Mtor and Wipi1 in lens fiber samples compared to lens epithelium at E13. These changes were not detected in the mouse data, most likely due to the differences between the stages of lens cell differentiation between the E13 chicken and newborn (P1) mouse lenses. The E13 chicken lens fiber portions establish

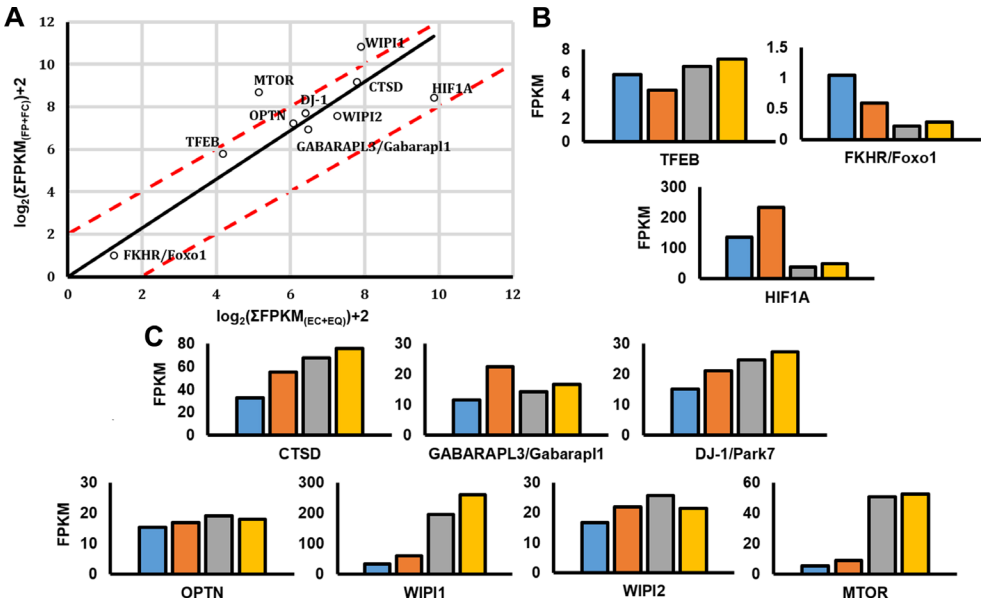

Figure 10. Dynamics of autophagy gene expression in four compartments of E13 embryonic chicken lenses **A**: Summary of expression data for E13 chicken lenses. **B**: Tfeb, Foxo1, and Hif1a. **C**: Ctsd, Gabarapl3 (homolog of Gaparapl1), Park7 (DJ-1), Optn, Wipi1, Wipi2, and Mtor. Central anterior epithelium (blue), equatorial epithelium (orange), cortical fibers (gray), and central fiber core (yellow).

an organelle-free zone, while in newborn mouse lenses, the organelle-free zone is already established. We conclude that both mouse and chicken lenses express cohorts of genes implicated in autophagy, and the high abundance of some of their transcripts points to specific functions in lens homeostasis and organelle degradation and identifies candidate genes for functional studies in both systems.

Genome-wide studies of lens chromatin and gene regulation during lens differentiation: Taken together, the present study establishes that crystallins are among a sparse group of the most abundantly expressed genes in mammalian tissues and organs. Their expression levels are further increased by 2–3 orders of magnitude in lens fibers relative to lens epithelium, where, for example, αA-crystallin is already abundantly expressed (at least 1,000-fold relative to the median expression level). Based on these data, it appears that a significant portion of the transcriptional apparatus is committed to transcribe crystallin genes, as evidenced by the high density of pol-II across the coding exons, introns and extended 3'-UTRs. In addition, crystallin loci show increased "open" chromatin accessibility, as evaluated by FAIRE-seq. These findings suggest several possible models, for example, formation of 3D transcriptional factories in which multiple crystallin loci are physically tethered in the 3D-space of the nuclei [116]. Finally, transcriptional machinery can be visualized through high-resolution two-photon microscopy of fluorescently tagged proteins [117,118]. Thus, the crystallin loci can be used as excellent sites to study the pol II elongation rate, nucleosome dynamics, and transcriptional termination. All these models are testable, and ongoing experiments are focused on addressing these outstanding questions.

Although RNA studies can be conducted using 10,000 to 100,000 cells and using single cells following amplification [119], the main limitation of chromatin studies is that while for special applications, 10,000 cells are sufficient, the majority of experiments require large amounts of materials (e.g., 20–300 lenses) and high-quality antibodies. The present studies represent a mixture of primary lens cells, and additional studies will be required to assess chromatin interaction in lens epithelium and lens fibers. It is also noteworthy that the cross-linking stabilizes actual protein-DNA interactions but does not reveal dynamics of transcription factor–DNA interactions in the specific nucleosome or linker region. Nevertheless, the RNA-seq studies were conducted with isolated lens epithelium and lens fibers and aid in the interpretation of chromatin data obtained from the whole lens.

APPENDIX 1. FUNCTIONAL ANNOTATION OF GENES NEXT TO FAIRE-SEQ PEAKS IN SUPER-ENHANCERS.

A) Top enriched Gene Ontology (GO: biologic process) terms. B) Top enriched mouse phenotypes. The enrichment analysis was performed by the GREAT software. To access the data, click or select the words "Appendix 1."

ACKNOWLEDMENTS

This work was supported by NIH grants R01 EY012200 (AC), EY014237 (AC), EY013022 (MK), and R21 MH099452 (DZ), and by unrestricted departmental grant from Research to Prevent Blindness, Inc. to the Department of Ophthalmology and Visual Sciences. We thank the Einstein Genomics and Epigenomics and Proteomics Shared Facilities for their services. Data in this paper are from a thesis submitted in partial fulfillment of the requirements for the Degree of Doctor of Philosophy in the Graduate Division of Medical Sciences, Albert Einstein College of Medicine, Yeshiva University (JS).

REFERENCES

1. Hawkins RD, Hon GC, Ren B. Next-generation genomics: an integrative approach. Nat Rev Genet 2010; 11:476-86. [PMID: 20531367].
2. Zhou VW, Goren A, Bernstein BE. Charting histone modifications and the functional organization of mammalian genomes. Nat Rev Genet 2011; 12:7-18. [PMID: 21116306].
3. Tsompana M, Buck MJ. Chromatin accessibility: a window into the genome. Epigenetics Chromatin 2014; 7:33-[PMID: 25473421].
4. Sun J, Rockowitz S, Xie Q, Ashery-Padan R, Zheng D, Cvekl A. Identification of *in vivo* DNA-binding mechanisms of Pax6 and reconstruction of Pax6-dependent gene regulatory networks during forebrain and lens development. Nucleic Acids Res 2015;43:6827-46. [PMID: 26138486].
5. Hoang TV, Kumar PK, Sutharzan S, Tsonis PA, Liang C, Robinson ML. Comparative transcriptome analysis of epithelial and fiber cells in newborn mouse lenses with RNA sequencing. Mol Vis 2014; 20:1491-517. [PMID: 25489224].
6. Chauss D, Basu S, Rajakaruna S, Gau V, Anastas S, Brennan LA, Hejtmancik JF, Menko AS, Kantorow M. Differentiation state-specific mitochondrial dynamic regulatory networks are revealed by global transcriptional analysis of the developing chicken lens. G3 (Bethesda) 2014; 4:1515-27. [PMID: 2492858]
7. Lachke SA, Ho JW, Kryukov GV, O'Connell DJ, Aboukhalil A, Bulyk ML, Park PJ, Maas RL. iSyTE: integrated Systems Tool for Eye gene discovery. Invest Ophthalmol Vis Sci 2012; 53:1617-27. [PMID: 22323457].
8. Gaulton KJ, Nammo T, Pasquali L, Simon JM, Giresi PG, Fogarty MP, Panhuis TM, Mieczkowski P, Secchi A, Bosco D, Berney T, Montanya E, Mohlke KL, Lieb JD, Ferrer J. A map of open chromatin in human pancreatic islets. Nat Genet 2010; 42:255-9. [PMID: 20118932].
9. Sheffield NC, Thurman RE, Song L, Safi A, Stamatoyannopoulos JA, Lenhard B, Crawford GE, Furey TS. Patterns of regulatory activity across diverse human cell types predict tissue identity, transcription factor binding, and long-range interactions. Genome Res 2013; 23:777-88. [PMID: 23482648].
10. Murtha M, Strino F, Tokcaer-Keskin Z, Sumru Bayin N, Shalabi D, Xi X, Kluger Y, Dailey L. Comparative FAIRE-seq analysis reveals distinguishing features of the chromatin structure of ground state- and primed-pluripotent cells. Stem Cells 2015; 33:378-91. [PMID: 25335464].
11. Thurman RE, Rynes E, Humbert R, Vierstra J, Maurano MT, Haugen E, Sheffield NC, Stergachis AB, Wang H, Vernot B, Garg K, John S, Sandstrom R, Bates D, Boatman L, Canfield TK, Diegel M, Dunn D, Ebersol AK, Frum T, Giste E, Johnson AK, Johnson EM, Kutyavin T, Lajoie B, Lee BK, Lee K, London D, Lotakis D, Neph S, Neri F, Nguyen ED, Qu H, Reynolds AP, Roach V, Safi A, Sanchez ME, Sanyal A, Shafer A, Simon JM, Song L, Vong S, Weaver M, Yan Y, Zhang Z, Zhang Z, Lenhard B, Tewari M, Dorschner MO, Hansen RS, Navas PA, Stamatoyannopoulos G, Iyer VR, Lieb JD, Sunyaev SR, Akey JM, Sabo PJ, Kaul R, Furey TS, Dekker J, Crawford GE, Stamatoyannopoulos JA. The accessible chromatin landscape of the human genome. Nature 2012; 489:75-82. [PMID: 22955617].
12. Ponts N, Harris EY, Prudhomme J, Wick I, Eckhardt-Ludka C, Hicks GR, Hardiman G, Lonardi S, Le Roch KG. Nucleosome landscape and control of transcription in the human malaria parasite. Genome Res 2010; 20:228-38. [PMID: 20054063].
13. Buenrostro JD, Giresi PG, Zaba LC, Chang HY, Greenleaf WJ. Transposition of native chromatin for fast and sensitive epigenomic profiling of open chromatin, DNA-binding proteins and nucleosome position. Nat Methods 2013; 10:1213-8. [PMID: 24097267].
14. Davie K, Jacobs J, Atkins M, Potier D, Christiaens V, Halder G, Aerts S. Discovery of transcription factors and regulatory regions driving in vivo tumor development by ATAC-seq and FAIRE-seq open chromatin profiling. PLoS Genet 2015; 11:e1004994-[PMID: 25679813].
15. Yaragatti M, Basilico C, Dailey L. Identification of active transcriptional regulatory modules by the functional assay of DNA from nucleosome-free regions. Genome Res 2008; 18:930-8. [PMID: 18441229].
16. Lovicu FJ, McAvoy JW. Growth factor regulation of lens development. Dev Biol 2005; 280:1-14. [PMID: 15766743].
17. Bassnett S. On the mechanism of organelle degradation in the vertebrate lens. Exp Eye Res 2009; 88:133-9. [PMID: 18840431].
18. Cvekl A, Ashery-Padan R. The cellular and molecular mechanisms of vertebrate lens development. Development 2014; 141:4432-47. [PMID: 25406393].
19. Piatigorsky J. Lens differentiation in vertebrates. A review of cellular and molecular features. Differentiation 1981; 19:134-53. [PMID: 7030840].
20. Cvekl A, Yang Y, Chauhan BK, Cveklova K. Regulation of gene expression by Pax6 in ocular cells: a case of tissue-preferred expression of crystallins in lens. Int J Dev Biol 2004; 48:829-44. [PMID: 15558475].

21. Cvekl A, Duncan MK. Genetic and epigenetic mechanisms of gene regulation during lens development. Prog Retin Eye Res 2007; 26:555-97. [PMID: 17905638].

22. Trapnell C, Pachter L, Salzberg SL. TopHat: discovering splice junctions with RNA-Seq. Bioinformatics 2009; 25:1105-11. [PMID: 19289445].

23. Trapnell C, Salzberg SL. How to map billions of short reads onto genomes. Nat Biotechnol 2009; 27:455-7. [PMID: 19430453].

24. Roberts A, Pimentel H, Trapnell C, Pachter L. Identification of novel transcripts in annotated genomes using RNA-Seq. Bioinformatics 2011; 27:2325-9. [PMID: 21697122].

25. Mortazavi A, Williams BA, McCue K, Schaeffer L, Wold B. Mapping and quantifying mammalian transcriptomes by RNA-Seq. Nat Methods 2008; 5:621-8. [PMID: 18516045].

26. Giresi PG, Kim J, McDaniell RM, Iyer VR, Lieb JD. FAIRE (Formaldehyde-Assisted Isolation of Regulatory Elements) isolates active regulatory elements from human chromatin. Genome Res 2007; 17:877-85. [PMID: 17179217].

27. Langmead B, Trapnell C, Pop M, Salzberg SL. Ultrafast and memory-efficient alignment of short DNA sequences to the human genome. Genome Biol 2009; 10:R25-[PMID: 19261174].

28. Zhang Y, Liu T, Meyer CA, Eeckhoute J, Johnson DS, Bernstein BE, Nusbaum C, Myers RM, Brown M, Li W, Liu XS. Model-based analysis of ChIP-Seq (MACS). Genome Biol 2008; 9:R137-[PMID: 18798982].

29. Kim H, Toyofuku Y, Lynn FC, Chak E, Uchida T, Mizukami H, Fujitani Y, Kawamori R, Miyatsuka T, Kosaka Y, Yang K, Honig G, van der Hart M, Kishimoto N, Wang J, Yagihashi S, Tecott LH, Watada H, German MS. Serotonin regulates pancreatic beta cell mass during pregnancy. Nat Med 2010; 16:804-8. [PMID: 20581837].

30. Bergsland M, Ramskold D, Zaouter C, Klum S, Sandberg R, Muhr J. Sequentially acting Sox transcription factors in neural lineage development. Genes Dev 2011; 25:2453-64. [PMID: 22085726].

31. Lara-Astiaso D, Weiner A, Lorenzo-Vivas E, Zaretsky I, Jaitin DA, David E, Keren-Shaul H, Mildner A, Winter D, Jung S, Friedman N, Amit I. Immunogenetics. Chromatin state dynamics during blood formation. Science 2014; 345:943-9. [PMID: 25103404].

32. Rodríguez-Seguel E, Mah N, Naumann H, Pongrac IM, Cerda-Esteban N, Fontaine JF, Wang Y, Chen W, Andrade-Navarro MA, Spagnoli FM. Mutually exclusive signaling signatures define the hepatic and pancreatic progenitor cell lineage divergence. Genes Dev 2013; 27:1932-46. [PMID: 24013505].

33. Wigle JT, Chowdhury K, Gruss P, Oliver G. Prox1 function is crucial for mouse lens-fibre elongation. Nat Genet 1999; 21:318-22. [PMID: 10080188].

34. Cui W, Tomarev SI, Piatigorsky J, Chepelinsky AB, Duncan MK. Mafs, Prox1, and Pax6 can regulate chicken βB1-crystallin gene expression. J Biol Chem 2004; 279:11088-95. [PMID: 14707122].

35. Westmoreland JJ, Kilic G, Sartain C, Sirma S, Blain J, Rehg J, Harvey N, Sosa-Pineda B. Pancreas-specific deletion of Prox1 affects development and disrupts homeostasis of the exocrine pancreas. Gastroenterology 2012; 142:999-1009. [PMID: 22178591].

36. Kim JI, Li T, Ho IC, Grusby MJ, Glimcher LH. Requirement for the c-Maf transcription factor in crystallin gene regulation and lens development. Proc Natl Acad Sci USA 1999; 96:3781-5. [PMID: 10097114].

37. Kawauchi S, Takahashi S, Nakajima O, Ogino H, Morita M, Nishizawa M, Yasuda K, Yamamoto M. Regulation of lens fiber cell differentiation by transcription factor c-Maf. J Biol Chem 1999; 274:19254-60. [PMID: 10383433].

38. Ring BZ, Cordes SP, Overbeek PA, Barsh GS. Regulation of mouse lens fiber cell development and differentiation by the Maf gene. Development 2000; 127:307-17. [PMID: 10603348].

39. Chauhan BK, Yang Y, Cveklova K, Cvekl A. Functional interactions between alternatively spliced forms of Pax6 in crystallin gene regulation and in haploinsufficiency. Nucleic Acids Res 2004; 32:1696-709. [PMID: 15020706].

40. Yang Y, Chauhan BK, Cveklova K, Cvekl A. Transcriptional regulation of mouse αB- and γF-crystallin genes in lens: opposite promoter-specific interactions between Pax6 and large Maf transcription factors. J Mol Biol 2004; 344:351-68. [PMID: 15522290].

41. Yang Y, Cvekl A. Tissue-specific regulation of the mouse αA-crystallin gene in lens via recruitment of Pax6 and c-Maf to its promoter. J Mol Biol 2005; 351:453-69. [PMID: 16023139].

42. Xie Q, Cvekl A. The orchestration of mammalian tissue morphogenesis through a series of coherent feed-forward loops. J Biol Chem 2011; 286:43259-71. [PMID: 21998302].

43. Takeuchi T, Kudo T, Ogata K, Hamada M, Nakamura M, Kito K, Abe Y, Ueda N, Yamamoto M, Engel JD, Takahashi S. Neither MafA/L-Maf nor MafB is essential for lens development in mice. Genes Cells 2009; 14:941-7. [PMID: 19624757].

44. Sander M, Neubuser A, Kalamaras J, Ee HC, Martin GR, German MS. Genetic analysis reveals that PAX6 is required for normal transcription of pancreatic hormone genes and islet development. Genes Dev 1997; 11:1662-73. [PMID: 9224716].

45. Planque N, Leconte L, Coquelle FM, Benkhelifa S, Martin P, Felder-Schmittbuhl MP, Saule S. Interaction of Maf transcription factors with Pax-6 results in synergistic activation of the glucagon promoter. J Biol Chem 2001; 276:35751-60. [PMID: 11457839].

46. Ritz-Laser B, Estreicher A, Klages N, Saule S, Philippe J. Pax-6 and Cdx-2/3 interact to activate glucagon gene expression on the G1 control element. J Biol Chem 1999; 274:4124-32. [PMID: 9933606].

47. Andersen FG, Heller RS, Petersen HV, Jensen J, Madsen OD, Serup P. Pax6 and Cdx2/3 form a functional complex on the rat glucagon gene promoter G1-element. FEBS Lett 1999; 445:306-10. [PMID: 10094478].

48. Grzeskowiak R, Amin J, Oetjen E, Knepel W. Insulin responsiveness of the glucagon gene conferred by interactions between proximal promoter and more distal enhancer-like elements involving the paired-domain transcription factor Pax6. J Biol Chem 2000; 275:30037-45. [PMID: 10862760].

49. Olbrot M, Rud J, Moss LG, Sharma A. Identification of β-cell-specific insulin gene transcription factor RIPE3b1 as mammalian MafA. Proc Natl Acad Sci USA 2002; 99:6737-42. [PMID: 12011435].

50. Raum JC, Hunter CS, Artner I, Henderson E, Guo M, Elghazi L, Sosa-Pineda B, Ogihara T, Mirmira RG, Sussel L, Stein R. Islet β-cell-specific MafA transcription requires the 5′-flanking conserved region 3 control domain. Mol Cell Biol 2010; 30:4234-44. [PMID: 20584984].

51. Artner I, Le Lay J, Hang Y, Elghazi L, Schisler JC, Henderson E, Sosa-Pineda B, Stein R. MafB: an activator of the glucagon gene expressed in developing islet α- and β-cells. Diabetes 2006; 55:297-304. [PMID: 16443760].

52. Artner I, Blanchi B, Raum JC, Guo M, Kaneko T, Cordes S, Sieweke M, Stein R. MafB is required for islet beta cell maturation. Proc Natl Acad Sci USA 2007; 104:3853-8. [PMID: 17360442].

53. Kataoka K, Shioda S, Ando K, Sakagami K, Handa H, Yasuda K. Differentially expressed Maf family transcription factors, c-Maf and MafA, activate glucagon and insulin gene expression in pancreatic islet α- and β-cells. J Mol Endocrinol 2004; 32:9-20. [PMID: 14765989].

54. Clements J, Hens K, Francis C, Scellens A, Callaerts P. Conserved role for the Drosophila Pax6 homolog Eyeless in differentiation and function of insulin-producing neurons. Proc Natl Acad Sci USA 2008; 105:16183-8. [PMID: 18852455].

55. Gopal-Srivastava R, Haynes JI 2nd, Piatigorsky J. Regulation of the murine αB-crystallin/small heat shock protein gene in cardiac muscle. Mol Cell Biol 1995; 15:7081-90. [PMID: 8524275].

56. Fort PE, Freeman WM, Losiewicz MK, Singh RS, Gardner TW. The retinal proteome in experimental diabetic retinopathy: up-regulation of crystallins and reversal by systemic and periocular insulin. Mol Cell Proteomics 2009; 8:767-79. [PMID: 19049959].

57. Reddy VS, Raghu G, Reddy SS, Pasupulati AK, Suryanarayana P, Reddy GB. Response of small heat shock proteins in diabetic rat retina. Invest Ophthalmol Vis Sci 2013; 54:7674-82. [PMID: 24159092].

58. Fujimoto M, Izu H, Seki K, Fukuda K, Nishida T, Yamada S, Kato K, Yonemura S, Inouye S, Nakai A. HSF4 is required for normal cell growth and differentiation during mouse lens development. EMBO J 2004; 23:4297-306. [PMID: 15483628].

59. Sims RJ 3rd, Belotserkovskaya R, Reinberg D. Elongation by RNA polymerase II: the short and long of it. Genes Dev 2004; 18:2437-68. [PMID: 15489290].

60. Li G, Reinberg D. Chromatin higher-order structures and gene regulation. Curr Opin Genet Dev 2011; 21:175-86. [PMID: 21342762].

61. Whyte WA, Orlando DA, Hnisz D, Abraham BJ, Lin CY, Kagey MH, Rahl PB, Lee TI, Young RA. Master transcription factors and mediator establish super-enhancers at key cell identity genes. Cell 2013; 153:307-19. [PMID: 23582322].

62. McLean CY, Bristor D, Hiller M, Clarke SL, Schaar BT, Lowe CB, Wenger AM, Bejerano G. GREAT improves functional interpretation of cis-regulatory regions. Nat Biotechnol 2010; 28:495-501. [PMID: 20436461].

63. Pevny LH, Nicolis SK. Sox2 roles in neural stem cells. Int J Biochem Cell Biol 2010; 42:421-4. [PMID: 19733254].

64. Yang Y, Stopka T, Golestaneh N, Wang Y, Wu K, Li A, Chauhan BK, Gao CY, Cveklova K, Duncan MK, Pestell RG, Chepelinsky AB, Skoultchi AI, Cvekl A. Regulation of αA-crystallin via Pax6, c-Maf, CREB and a broad domain of lens-specific chromatin. EMBO J 2006; 25:2107-18. [PMID: 16675956].

65. He S, Pirity MK, Wang WL, Wolf L, Chauhan BK, Cveklova K, Tamm ER, Ashery-Padan R, Metzger D, Nakai A, Chambon P, Zavadil J, Cvekl A. Chromatin remodeling enzyme Brg1 is required for mouse lens fiber cell terminal differentiation and its denucleation. Epigenetics Chromatin 2010; 3:21-[PMID: 21118511].

66. Wolf L, Yang Y, Wawrousek E, Cvekl A. Transcriptional regulation of mouse αA-crystallin gene in a 148kb Cryaa BAC and its derivates. BMC Dev Biol 2008; 8:88-[PMID: 18803847].

67. Swamynathan SK, Piatigorsky J. Orientation-dependent influence of an intergenic enhancer on the promoter activity of the divergently transcribed mouse Shsp/αB-crystallin and Mkbp/HspB2 genes. J Biol Chem 2002; 277:49700-6. [PMID: 12403771].

68. Swamynathan SK, Piatigorsky J. Regulation of the mouse αB-crystallin and MKBP/HspB2 promoter activities by shared and gene specific intergenic elements: the importance of context dependency. Int J Dev Biol 2007; 51:689-700. [PMID: 17939115].

69. Haynes JI 2nd, Duncan MK, Piatigorsky J. Spatial and temporal activity of the αB-crystallin/small heat shock protein gene promoter in transgenic mice. Dev Dyn 1996; 207:75-88. [PMID: 8875078].

70. van Leen RW, van Roozendaal KE, Lubsen NH, Schoenmakers JG. Differential expression of crystallin genes during development of the rat eye lens. Dev Biol 1987; 120:457-64. [PMID: 3030857].

71. Ragoczy T, Bender MA, Telling A, Byron R, Groudine M. The locus control region is required for association of the murine β-globin locus with engaged transcription factories

during erythroid maturation. Genes Dev 2006; 20:1447-57. [PMID: 16705039].

72. de Laat W, Grosveld F. Spatial organization of gene expression: the active chromatin hub. Chromosome Res 2003; 11:447-59. [PMID: 12971721].

73. Cvekl A, Mitton KP. Epigenetic regulatory mechanisms in vertebrate eye development and disease. Heredity 2010; 105:135-51. [PMID: 20179734].

74. Manuel MN, Mi D, Mason JO, Price DJ. Regulation of cerebral cortical neurogenesis by the Pax6 transcription factor. Front Cell Neurosci 2015; 9:70-[PMID: 25805971].

75. Tanaka K, Chiba T. The proteasome: a protein-destroying machine. Genes Cells 1998; 3:499-510. [PMID: 9797452].

76. Firtina Z, Duncan MK. Unfolded Protein Response (UPR) is activated during normal lens development. Gene Expr Patterns 2011; 11:135-43. [PMID: 21044701].

77. Antosova B, Smolikova J, Borkovcova R, Strnad H, Lachova J, Machon O, Kozmik Z. Ectopic activation of Wnt/beta-catenin signaling in lens fiber cells results in cataract formation and aberrant fiber cell differentiation. PLoS ONE 2013; 8:e78279-[PMID: 24205179].

78. Sugiyama Y, Lovicu FJ, McAvoy JW. Planar cell polarity in the mammalian eye lens. Organogenesis 2011; 7:191-201. [PMID: 22027540].

79. West-Mays JA, Zhang J, Nottoli T, Hagopian-Donaldson S, Libby D, Strissel KJ, Williams T. AP-2α transcription factor is required for early morphogenesis of the lens vesicle. Dev Biol 1999; 206:46-62. [PMID: 9918694].

80. Blixt A, Mahlapuu M, Aitola M, Pelto-Huikko M, Enerback S, Carlsson P. A forkhead gene, FoxE3, is essential for lens epithelial proliferation and closure of the lens vesicle. Genes Dev 2000; 14:245-54. [PMID: 10652278].

81. Jing Z, Gangalum RK, Bhat AM, Nagaoka Y, Jiang M, Bhat SP. HSF4 mutation p.Arg116His found in age-related cataracts and in normal populations produces childhood lamellar cataract in transgenic mice. Hum Mutat 2014; 35:1068-71. [PMID: 24975927].

82. Somasundaram T, Bhat SP. Developmentally dictated expression of heat shock factors: exclusive expression of HSF4 in the postnatal lens and its specific interaction with αB-crystallin heat shock promoter. J Biol Chem 2004; 279:44497-503. [PMID: 15308659].

83. Cadigan KM, Waterman ML. TCF/LEFs and Wnt signaling in the nucleus. Cold Spring Harb Perspect Biol 2012; 4:[PMID: 23024173].

84. Kamachi Y, Uchikawa M, Tanouchi A, Sekido R, Kondoh H. Pax6 and SOX2 form a co-DNA-binding partner complex that regulates initiation of lens development. Genes Dev 2001; 15:1272-86. [PMID: 11358870].

85. Donner AL, Episkopou V, Maas RL. Sox2 and Pou2f1 interact to control lens and olfactory placode development. Dev Biol 2007; 303:784-99. [PMID: 17140559].

86. Smith AN, Miller LA, Radice G, Ashery-Padan R, Lang RA. Stage-dependent modes of Pax6-Sox2 epistasis regulate lens development and eye morphogenesis. Development 2009; 136:2977-85. [PMID: 19666824].

87. Episkopou V. SOX2 functions in adult neural stem cells. Trends Neurosci 2005; 28:219-21. [PMID: 15866195].

88. Uchikawa M, Ishida Y, Takemoto T, Kamachi Y, Kondoh H. Functional analysis of chicken Sox2 enhancers highlights an array of diverse regulatory elements that are conserved in mammals. Dev Cell 2003; 4:509-19. [PMID: 12689590].

89. Wurm A, Sock E, Fuchshofer R, Wegner M, Tamm ER. Anterior segment dysgenesis in the eyes of mice deficient for the high-mobility-group transcription factor Sox11. Exp Eye Res 2008; 86:895-907. [PMID: 18423449].

90. Shaham O, Gueta K, Mor E, Oren-Giladi P, Grinberg D, Xie Q, Cvekl A, Shomron N, Davis N, Keydar-Prizant M, Raviv S, Pasmanik-Chor M, Bell RE, Levy C, Avellino R, Banfi S, Conte I, Ashery-Padan R. Pax6 regulates gene expression in the vertebrate lens through miR-204. PLoS Genet 2013; 9:e1003357-[PMID: 23516376].

91. Han G, Gupta SD, Gable K, Niranjanakumari S, Moitra P, Eichler F, Brown RH Jr, Harmon JM, Dunn TM. Identification of small subunits of mammalian serine palmitoyltransferase that confer distinct acyl-CoA substrate specificities. Proc Natl Acad Sci USA 2009; 106:8186-8191. [PMID: 19416851].

92. Wang Y, Lin L, Lai H, Parada LF, Lei L. Transcription factor Sox11 is essential for both embryonic and adult neurogenesis. Dev Dyn 2013; 242:638-53. [PMID: 23483698].

93. Wolf L, Harrison W, Huang J, Xie Q, Xiao N, Sun J, Kong L, Lachke SA, Kuracha MR, Govindarajan V, Brindle PK, Ashery-Padan R, Beebe DC, Overbeek PA, Cvekl A. Histone posttranslational modifications and cell fate determination: lens induction requires the lysine acetyltransferases CBP and p300. Nucleic Acids Res 2013; 41:10199-214. [PMID: 24038357].

94. Yang Y, Wolf LV, Cvekl A. Distinct embryonic expression and localization of CBP and p300 histone acetyltransferases at the mouse αA-crystallin locus in lens. J Mol Biol 2007; 369:917-26. [PMID: 17467007].

95. He S, Cvekl A. Focus on molecules: Brg1: a range of functions during eye development. Exp Eye Res 2012; 103:117-8. [PMID: 21963585].

96. Basu S, Rajakaruna S, Reyes B, Van Bockstaele E, Menko AS. Suppression of MAPK/JNK-MTORC1 signaling leads to premature loss of organelles and nuclei by autophagy during terminal differentiation of lens fiber cells. Autophagy 2014; 10:1193-211. [PMID: 24813396].

97. Costello MJ, Brennan LA, Basu S, Chauss D, Mohamed A, Gilliland KO, Johnsen S, Menko AS, Kantorow M. Autophagy and mitophagy participate in ocular lens organelle degradation. Exp Eye Res 2013; 116:141-50. [PMID: 24012988].

98. Nishimoto S, Kawane K, Watanabe-Fukunaga R, Fukuyama H, Ohsawa Y, Uchiyama Y, Hashida N, Ohguro N, Tano Y, Morimoto T, Fukuda Y, Nagata S. Nuclear cataract caused by a lack of DNA degradation in the mouse eye lens. Nature 2003; 424:1071-4. [PMID: 12944971].

99. Guo W, Shang F, Liu Q, Urim L, West-Mays J, Taylor A. Differential regulation of components of the ubiquitin-proteasome pathway during lens cell differentiation. Invest Ophthalmol Vis Sci 2004; 45:1194-201. [PMID: 15037588].

100. Caceres A, Shang F, Wawrousek E, Liu Q, Avidan O, Cvekl A, Yang Y, Haririnia A, Storaska A, Fushman D, Kuszak J, Dudek E, Smith D, Taylor A. Perturbing the ubiquitin pathway reveals how mitosis is hijacked to denucleate and regulate cell proliferation and differentiation in vivo. PLoS ONE 2010; 5:e13331-[PMID: 20975996].

101. Yamada T, Hara S, Tamai M. Immunohistochemical localization of cathepsin D in ocular tissues. Invest Ophthalmol Vis Sci 1990; 31:1217-23. [PMID: 2194988].

102. Yao J, Jia L, Khan N, Lin C, Mitter SK, Boulton ME, Dunaief JL, Klionsky DJ, Guan JL, Thompson DA, Zacks DN. Deletion of autophagy inducer RB1CC1 results in degeneration of the retinal pigment epithelium. Autophagy 2015; 11:939-53. [PMID: 26075877].

103. Le Grand JN, Chakrama FZ, Seguin-Py S, Fraichard A, Delage-Mourroux R, Jouvenot M, Boyer-Guittaut M. GABARAPL1 (GEC1): original or copycat? Autophagy 2011; 7:1098-107. [PMID: 21597319].

104. Rimessi A, Bonora M, Marchi S, Patergnani S, Marobbio CM, Lasorsa FM, Pinton P. Perturbed mitochondrial Ca2+ signals as causes or consequences of mitophagy induction. Autophagy 2013; 9:1677-86. [PMID: 24121707].

105. Gomes LC, Scorrano L. High levels of Fis1, a pro-fission mitochondrial protein, trigger autophagy. Biochim Biophys Acta 2008; 1777:860-6. [PMID: 18515060].

106. Zhang Q, Wu J, Wu R, Ma J, Du G, Jiao R, Tian Y, Zheng Z, Yuan Z. DJ-1 promotes the proteasomal degradation of Fis1: implications of DJ-1 in neuronal protection. Biochem J 2012; 447:261-9. [PMID: 22871147].

107. Majcher V, Goode A, James V, Layfield R. Autophagy receptor defects and ALS-FTLD. Mol Cell Neurosci 2015; 66:43-52. [PMID: 25683489].

108. Müller AJ, Proikas-Cezanne T. Function of human WIPI proteins in autophagosomal rejuvenation of endomembranes? FEBS Lett 2015; 589:1546-51. [PMID: 25980605].

109. Codogno P, Meijer AJ. Autophagy and signaling: their role in cell survival and cell death. Cell Death Differ 2005; 12:1509-18. [PMID: 16247498].

110. Laplante M, Sabatini DM. mTOR signaling in growth control and disease. Cell 2012; 149:274-93. [PMID: 22500797].

111. Sardiello M, Palmieri M, di Ronza A, Medina DL, Valenza M, Gennarino VA, Di Malta C, Donaudy F, Embrione V, Polishchuk RS, Banfi S, Parenti G, Cattaneo E, Ballabio A. A gene network regulating lysosomal biogenesis and function. Science 2009; 325:473-7. [PMID: 19556463].

112. Lapierre LR, Kumsta C, Sandri M, Ballabio A, Hansen M. Transcriptional and epigenetic regulation of autophagy in aging. Autophagy 2015; 11:867-80. [PMID: 25836756].

113. Hubbi ME, Gilkes DM, Hu H. Kshitiz, Ahmed I, Semenza GL. Cyclin-dependent kinases regulate lysosomal degradation of hypoxia-inducible factor 1α to promote cell-cycle progression. Proc Natl Acad Sci USA 2014; 111:E3325-34. [PMID: 25071185].

114. Bellot G, Garcia-Medina R, Gounon P, Chiche J, Roux D, Pouyssegur J, Mazure NM. Hypoxia-induced autophagy is mediated through hypoxia-inducible factor induction of BNIP3 and BNIP3L via their BH3 domains. Mol Cell Biol 2009; 29:2570-81. [PMID: 19273585].

115. Zhao H, Yang Y, Rizo CM, Overbeek PA, Robinson ML. Insertion of a Pax6 consensus binding site into the αA-crystallin promoter acts as a lens epithelial cell enhancer in transgenic mice. Invest Ophthalmol Vis Sci 2004; 45:1930-9. [PMID: 15161860].

116. de Laat W, Dekker J. 3C-based technologies to study the shape of the genome. Methods 2012; 58:189-91. [PMID: 23199640].

117. Liu Z, Legant WR, Chen BC, Li L, Grimm JB, Lavis LD, Betzig E, Tjian R. 3D imaging of Sox2 enhancer clusters in embryonic stem cells. Elife. 2014; 3:e04236-[PMID: 25537195].

118. Chen J, Zhang Z, Li L, Chen BC, Revyakin A, Hajj B, Legant W, Dahan M, Lionnet T, Betzig E, Tjian R, Liu Z. Single-molecule dynamics of enhanceosome assembly in embryonic stem cells. Cell 2014; 156:1274-85. [PMID: 24630727].

119. Macaulay IC, Voet T. Single cell genomics: advances and future perspectives. PLoS Genet 2014; 10:e1004126-[PMID: 24497842].

120. Zhang H, Meltzer P, Davis S. RCircos: an R package for Circos 2D track plots. BMC Bioinformatics 2013; 14:244-[PMID: 23937229].

Articles are provided courtesy of Emory University and the Zhongshan Ophthalmic Center, Sun Yat-sen University, P.R. China. The print version of this article was created on 28 August 2015. This reflects all typographical corrections and errata to the article through that date. Details of any changes may be found in the online version of the article.